

## LA-UR-17-20385

Approved for public release; distribution is unlimited.

Title: Annealing of (DU-10Mo)-Zr Co-Rolled Foils

Author(s): Pacheco, Robin Montoya  
Alexander, David John  
McCabe, Rodney James  
Clarke, Kester Diederik  
Scott, Jeffrey E.  
Montalvo, Joel Dwayne  
Papin, Pallas

Intended for: Report

Issued: 2017-01-20

---

**Disclaimer:**

Los Alamos National Laboratory, an affirmative action/equal opportunity employer, is operated by the Los Alamos National Security, LLC for the National Nuclear Security Administration of the U.S. Department of Energy under contract DE-AC52-06NA25396. By approving this article, the publisher recognizes that the U.S. Government retains nonexclusive, royalty-free license to publish or reproduce the published form of this contribution, or to allow others to do so, for U.S. Government purposes. Los Alamos National Laboratory requests that the publisher identify this article as work performed under the auspices of the U.S. Department of Energy. Los Alamos National Laboratory strongly supports academic freedom and a researcher's right to publish; as an institution, however, the Laboratory does not endorse the viewpoint of a publication or guarantee its technical correctness.

## Annealing of (DU-10Mo)-Zr Co-Rolled Foils

---

Robin M. Pacheco, David J. Alexander, Rodney J. McCabe, Kester D. Clarke<sup>1</sup>,  
Jeffrey E. Scott, J.D. Montalvo, Pallas A. Papin<sup>2</sup>

Los Alamos National Laboratory,  
Sigma Division,  
Los Alamos, New Mexico, 87545

<sup>1</sup> George S. Ansell Department of Metallurgical and Materials Engineering,  
Colorado School of Mines, Golden, CO 80401,  
formerly LANL

<sup>2</sup> Retired, formerly LANL

## ABSTRACT

Producing uranium-10wt% molybdenum (DU-10Mo) foils to clad with Al first requires initial bonding of the DU-10Mo foil to zirconium (Zr) by hot rolling, followed by cold rolling to final thickness. Rolling often produces wavy (DU-10Mo)-Zr foils that should be flattened before further processing, as any distortions could affect the final alignment and bonding of the Al cladding to the Zr co-rolled surface layer; this bonding is achieved by a hot isostatic pressing (HIP) process. Distortions in the (DU-10Mo)-Zr foil may cause the fuel foil to press against the Al cladding and thus create thinner or thicker areas in the Al cladding layer during the HIP cycle. Post machining is difficult and risky at this stage in the process since there is a chance of hitting the DU-10Mo. Therefore, it is very important to establish a process to flatten and remove any waviness.

This study was conducted to determine if a simple annealing treatment could flatten wavy foils. Using the same starting material (i.e. DU-10Mo coupons of the same thickness), five different levels of hot rolling and cold rolling, combined with five different annealing treatments, were performed to determine the effect of these processing variables on flatness, bonding of layers, annealing response, microstructure, and hardness. The same final thickness was reached in all cases. Micrographs, textures, and hardness measurements were obtained for the various processing combinations. Based on these results, it was concluded that annealing at 650°C or higher is an effective treatment to appreciably reduce foil waviness.

**Keywords:** Uranium-10wt% molybdenum, zirconium, fuel foils, aluminum cladding, hot rolling, cold rolling, annealing, relative flatness, interfaces, interaction zone, composition gradients, recrystallization, texture, microhardness

## Table of Contents

<b>1.0</b>	<b>INTRODUCTION.....</b>	<b>4</b>
1.1	Importance of Research .....	4
1.2	General Techniques .....	5
<b>2.0</b>	<b>BACKGROUND .....</b>	<b>6</b>
2.1	DU-10Mo .....	6
2.2	HIP Processing .....	7
<b>3.0</b>	<b>EXPERIMENTAL PROCEDURE.....</b>	<b>8</b>
3.1	Rolling and Annealing .....	8
3.2	Microstructures and Microhardness .....	9
3.3	U, Mo, and Zr Profiles .....	10
<b>4.0</b>	<b>RESULTS &amp; DISCUSSION .....</b>	<b>10</b>
4.1	Flatness and Microstructure .....	10
4.2	U, Mo, and Zr Profiles .....	17
4.3	Microhardness .....	18
<b>4.0</b>	<b>CONCLUSIONS .....</b>	<b>19</b>
	<b>REFERENCES .....</b>	<b>20</b>
	<b>APPENDICES .....</b>	<b>21</b>

## 1.0 INTRODUCTION

### 1.1 Importance of Research

The U.S. Department of Energy National Nuclear Security Administration (DOE/NNSA) Office of Material Management and Minimization (M<sup>3</sup>) Reactor Conversion Program aims to reduce or eliminate the use of highly enriched uranium (HEU) dispersion fuels in high-powered research reactors in the United States by replacement with low enriched uranium (LEU) alloy monolithic fuel plates. Throughout the years, M<sup>3</sup> has converted or verified the shutdown of 87 research reactors worldwide, including 20 domestic facilities. Of the remaining domestic research reactors, five U.S. high performance research reactors (HPRRs) and one associated critical assembly will require a new high density LEU fuel and fabrication capability, which is currently under development, to convert. Existing qualified fuels do not meet the high fuel density requirements for the operation of these high-performance reactors, which include the Advanced Test Reactor (ATR) at Idaho National Laboratory, the High Flux Isotope Reactor (HFIR) at Oak Ridge National Laboratory, the University of Missouri Research Reactor (MURR), the Massachusetts Institute of Technology Reactor (MITR), and the Department of Commerce's National Bureau of Standards Reactor (NBSR). To maintain performance requirements, the Reactor Conversion program is developing a high density monolithic, rather than dispersion, plate fuel system which uses low enriched uranium-10wt% molybdenum (U-10Mo) foils coated with a layer of zirconium (Zr) and clad with 6061 aluminum (Al).

The baseline process for producing the U-10Mo fuel foils involves casting of the U-10Mo alloy, homogenization, sectioning of the cast ingot into appropriately sized coupons, and machining these coupons to the desired dimensions. After suitable cleaning of all components, the machined coupons are assembled into a steel can, along with thin foils of Zr on each face of the U-10Mo coupon. A parting agent is applied to the outer surfaces of the Zr foils, to prevent the Zr from bonding to the steel can during hot rolling. The assembled can is then welded shut along its edges to seal the U-10Mo and Zr foils inside and prevent their exposure to air during hot rolling. A large reduction in thickness by hot rolling is required to successfully bond the Zr to the U-10Mo fuel. The role of the Zr is to provide a diffusion barrier between the U-10Mo and an Al cladding layer that will be bonded to the fuel foil at a later stage in the fabrication process.

After hot rolling, the foil is removed from the can. Hot rolling results in a pebbled/orange peel exterior on the surface of the foils, and also does not permit precise control of the final foil thickness. Cold rolling must be performed to obtain flat, smooth foils with the desired final (total) thickness (Zr + U-10Mo + Zr). Although the intent of the hot and cold rolling is to produce flat, smooth foils, this is not always possible, and the foils may be bowed or rippled after rolling, either locally or over the length of the foil. These distortions may affect the final bonding of the Al cladding, which is achieved by a hot isostatic pressing (HIP) process. To save time, resources, and money, it would be very helpful if there was a process by which wavy foils could be flattened to remove or significantly reduce any ripples.

This study was performed to determine if a simple annealing treatment could flatten wavy foils. Preliminary results were reported previously<sup>1-2</sup>.

## 1.2 General Techniques

Hot rolling is a mechanism used to plastically deform a metal at a temperature above the recrystallization temperature. Typically, a metal will undergo hot rolling to permit large amounts of deformation which are achievable because of high dislocation mobility, and the soft and ductile state of the metal. The grains are small and refined due to the high temperature the metal is being hot rolled at. It is very common for hot rolled metals to exhibit a rough surface finish after hot rolling due to impurities of the cast material (gas porosity), friction of the rollers, longitudinal tension and slow cooling of the metal, inadequate bonding between layers of materials, induced internal stresses that lead to warping, formation of an oxide layer, or blisters caused by gas bubbles that formed on or beneath the surface during the high temperature processing<sup>3-6</sup>. Most surface defects can be removed by cold rolling.

Cold rolling is a mechanism used to harden a metal by plastically deforming it at lower temperatures relative to its melting point<sup>3</sup>. Cold rolling reduces the thickness, changes the microstructure, and enhances some properties. Microstructures often reveal grain elongation and orientation in the direction of cold working while the lattice structure exhibits an increase in dislocations with increased cold working. These changes can contribute to the enhancement in hardness and strength yet may cause a decrease in ductility (with increased cold working). As the amount of plastic deformation increases with increasing cold working, so does the stored strain energy. Strain energy is simply energy retained within the metal; it varies depending on composition, amount of deformation, and temperature of deformation. Strain energy increases with addition of alloying elements, great amounts of deformation, and lowering deformation temperatures. To reverse the effects of cold rolling and restore initial states the stored energy must be released. This is accomplished by annealing.

Annealing is the process of heat treating at high temperatures for a certain amount of time to remove the effects of cold working. Annealing takes place in three stages: recovery, recrystallization, and grain growth. When temperatures are low, recovery relieves strain energy by the movement of dislocations. Dislocations are rearranged and often reduced as sub grains begin to form. As temperatures rise, recrystallization occurs by forming new strain free, equiaxed grains. It is during the recrystallization stage that most mechanical properties can be restored to their pre-cold rolled states. Finally at a higher temperature or longer times of the annealing process, grain growth may occur as larger grains grow by consuming smaller grains. In cases where fine microstructures are desired, the heat treatment is cut short to prevent grain growth. Figure 1 shows schematically the stages of annealing and the changes of grains throughout these processes.

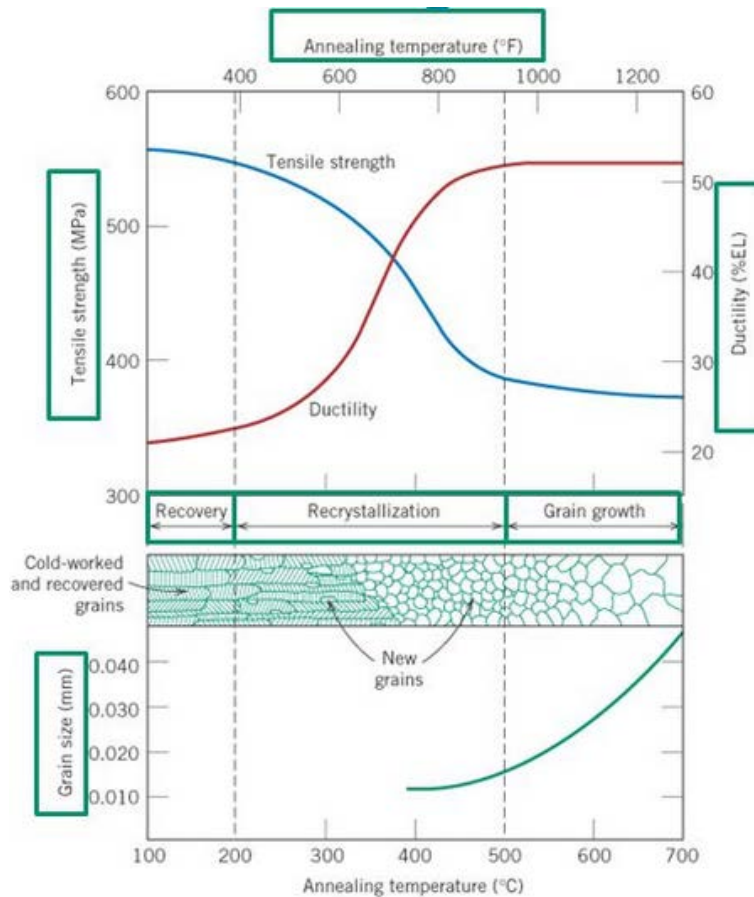


Figure 1: Transformations of grains as annealing temperature increases<sup>4</sup>. The top plot displays how mechanical properties change with increasing annealing temperatures.

## 2.0 BACKGROUND

### 2.1 DU-10Mo

Four 295 x 137 x 5 mm (11.6 x 5.4 x 0.20 in.) flat plate castings of depleted uranium, alloyed with 10 wt% molybdenum (DU-10Mo) were produced to supply material for this study. Figure 2 displays the setup used to make the plate castings. Graphite molds machined from HML graphite were coated with Type YK yttrium oxide mold coating, to prevent chemical reactions between the graphite and the molten uranium. Eight thermocouples were embedded in the mold to monitor the temperature during casting. For consistency, all castings had an average net weight of 4406 g, and an average elemental (DU) weight of 3966 g.





Figure 2: Casting setup. (a) Dimensions used for flat plates, (b) setup showing thermocouples, and (c) induction heating coils, top and bottom.

The typical procedure<sup>7</sup> for DU-10Mo plate casting is as follows:

- 1) Power crucible to 35 kW
- 2) Heat crucible to 1478°C (takes ~40 mins)
- 3) Cut crucible power to 5 kW and hold temperature at 1328°C until mold is at temperature
- 4) Power top coil to 30 kW (until mold temperature reaches 1300°C) and hold for ~25 min
- 5) Pour into mold
- 6) Turn off crucible and top coil after 1min.

The process takes ~1 hr. to complete. After the casting cooled, and was removed from the furnace and mold, the hot top was removed from the plate by electrical discharge machining (EDM). The plates were homogenized in vacuum for 4 hours at 1000°C then immediately oil quenched. Each plate was then sectioned by EDM into 6 coupons, nominally 96 x 67 mm (3.8 x 2.0 in.). The faces of each coupon were milled to a final coupon thickness of 3.8 mm (0.15 in.), with approximately equal amounts being removed from both faces; this required multiple passes on each face.

## 2.2 HIP Processing

Cladding aluminum to U-10Mo monolithic fuel plates is possible, and most practical, by the HIP bonding process. HIP stackups consist of the appropriate combination of strongbacks, fuel plate layers, Al cladding material, and parting agents. All parts are assembled in a stainless steel can that is hand welded shut to prevent component exposure during the HIP process. The welds sometimes cause distortions to the can making assembly and disassembly difficult. Further issues can arise if the (U-10Mo)-Zr foils are distorted and cannot be properly aligned with the Al cladding. This can cause the fuel foil to press unevenly against the Al cladding creating thinner and thicker areas in the cladding layer, as the Al layer softens during the high-temperature HIP cycle (560°C). Post machining should be avoided due to the risk of hitting the U-10Mo. Therefore, to ease the assembly and manufacturing process, it is best to begin with flat, straight (U-10Mo)-Zr foils for alignment, to allow the stackups to distribute uniform stresses along the assembled parts. Foils with wavy, pebbled/orange-peel surfaces may hinder flat, well-bonded, and overall good-quality monolithic fuel plates from being produced.

### 3.0 EXPERIMENTAL PROCEDURE

#### 3.1 Rolling and Annealing

After machining, the (DU-10Mo) coupons were cleaned and assembled into 135 x 105 x 12.7 mm (5.3 x 4.1 x 0.5 in.) mild steel cans. Each assembly began with the DU-10Mo coupon sandwiched between 0.25 mm (0.010 in.) thick Zr foils. This stack was then placed in a clean metal picture frame fixture where the through opening matched the thickness of the assembled coupon. A parting agent (Neolube 2: colloidal graphite in isopropanol) was applied to the outer surfaces of the Zr, to prevent the Zr from bonding to the steel can during hot rolling. Outer steel plates were clamped to the stack, to complete the assembly, which was then transferred to an argon glovebox for inert conditioning and welding. The clamps prevented misalignment during transfer and welding. The edges of the can were welded to seal the can and prevent exposure of the DU-10Mo and Zr to the atmosphere during hot rolling.

Table 1 gives the target levels of hot and cold rolling used in this study. True plane strains from 1.2 to 2.4 (based on an assumption of plane strain; i.e. no change in width during rolling), with an increment of 0.4, were chosen for the hot rolling. The levels of cold rolling were then adjusted, as necessary, to achieve the same final foil thickness (0.38 mm [0.015 in.]), in all cases. The 5% cold rolling was performed to determine whether some minimal level of cold rolling was acceptable for this process. True strains, calculated from the change in thickness only, are also included in the table. Annealing temperatures, from 550 to 750°C, in 50°C increments, were used. This range of temperatures includes the typical hot-rolling temperature in the baseline rolling process (650°C).

% Cold Roll	Final Foil Thickness (in.)	Hot-Rolled Foil Thickness (in.)	True Strain from Cold Rolling	True Strain (plane strain)		Initial Foil Thickness (in.)	Initial Can Thickness (in.)	% Hot Roll for Can	Can Thickness After HR (in.)	True strain from Hot Rolling	True Strain (plane strain)		Total Strain	Total Plane Strain
5	0.015	0.0158	0.051	0.059		0.170	0.490	90.7	0.0455	2.376	2.745		2.427	2.804
29	0.015	0.021	0.342	0.396		0.170	0.490	87.6	0.0609	2.085	2.408		2.427	2.804
50	0.015	0.030	0.693	0.801		0.170	0.490	82.4	0.0864	1.734	2.003		2.427	2.804
65	0.015	0.043	1.050	1.213		0.170	0.490	74.7	0.1235	1.378	1.592		2.428	2.805
75	0.015	0.060	1.386	1.601		0.170	0.490	64.7	0.1729	1.041	1.203		2.427	2.804

Table 1: Target hot and cold rolling levels. The % rolling is based on reduction of thickness and strains are negative (sign omitted for ease of table presentation).

The rolling cans were preheated to 650°C in an air furnace prior to hot rolling. Hot rolling was performed on a Bliss mill following the parameters in Table 1. The Bliss mill has a two high roll configuration. Each roll is 20 in. wide and 8.5 in. in diameter, and are preheated for use. An estimated roll speed of 20 fpm was used with a nominal reduction in thickness of ~10% per pass. The cans were reheated to 650°C after each rolling pass. Actual foil thickness could not be determined during hot rolling due to the presence of the steel can. Therefore the foil thickness was

calculated at each pass, based on the measured overall can thickness, assuming that foil and can deformation were proportional. Once hot rolling was complete, the cans were annealed in air for 30 minutes at 650°C, then cooled to room temperature. After cooling, the edges of the can were removed by power shearing, the foil was removed from the steel can, and then trimmed to shape and size. The actual foil thickness was measured at this point.

Cold rolling to the final thickness of 0.38 mm (0.015 in.) was performed using a Loewy mill. The Loewy mill has a four high roll configuration, with two backing rolls and two work rolls. The backing rolls are 20 in. wide and 18 in. in diameter, and the work rolls are 20 in. wide and 3.5 in. in diameter. An estimated roll speed of 5 fpm was used, with a nominal reduction in thickness of ~1% per pass.

The cold-rolled foils were trimmed to the required size and placed between weighted copper (Cu) plates for vacuum annealing. The intent of the weighted Cu plate was to ensure that the foils stayed flat during annealing. The total mass of the upper Cu plate and the extra weight was ~40 kg. Based on this setup, 0.25 lb/in<sup>2</sup> (0.0045 kg/mm) was applied to a set of 5 foils that were each 102 x 508 mm (4 x 20 in.). Vacuum annealing was performed for 1 hour at 550, 600, 650, 700, or 750°C, followed by oil quenching.

### 3.2 Microstructures and Microhardness

After annealing, samples were sectioned from each of the foils for metallographic examination. The samples were cold mounted and prepared following standard metallographic polishing procedures. The samples were etched with a 5% phosphoric acid solution to permit examination by light optical microscopy (LOM). Samples were also examined by scanning electron microscopy (SEM) which allowed the interface between the DU-10Mo and the Zr diffusion barrier to be examined at much higher magnification. Following LOM and SEM examinations, the samples were prepared for examination by electron backscatter diffraction (EBSD).

EBSD samples were first polished through 1 µm diamond followed by electropolishing for 4-5 minutes at 10 V using a stirred solution of 27.5% nitric acid, 27.5% ethylene glycol, and 45% ethanol (by volume). EBSD was performed on an FEI XL30 ESEM using an accelerating voltage of 25 kV, spot size of 5, and 100 µm aperture. EBSD scans were performed with a step size of 0.5 µm on areas at least 600 µm in length by the full width of the plates, which was around 350 µm. Micro-textures, represented as (100), (010), and (001) pole figures, were produced based on these scans. These are referred to as micro-textures because they are based on relatively limited areas and numbers of grains. The pole figure data are rotated such that the plate normal direction is normal to the pole figures and the A1 and A2 directions are consistent between the scans with A1 parallel to the rolling direction.

Two different types of microstructure scans are used to represent the data. The inverse pole figure (IPF) maps show the crystal direction parallel to the normal direction of the scan. Grain orientation spread (GOS) maps indicate the degree of orientation spread within individual grains and is calculated as the average mis-orientation between each scan point in a grain and the average orientation of the grain. This is a good indicator of whether a grain is recrystallized or not, with

recrystallized grains usually having a GOS of less than 1 degree. Non-recrystallized grains will have higher GOS values and will appear to be multicolored in the IPF maps.

Microhardness measurements were obtained from the same metallographic samples, along the transverse and longitudinal direction of the mounted samples using a Vickers tester with a 500 gf load and a 12 s dwell time. At least five measurements per sample were taken.

### **3.3 U, Mo and Zr Profiles**

Energy-dispersive spectroscopy (EDS) was performed using a CAMECA SX100 microprobe to measure the concentration of U, Mo, and Zr. Wavelength dispersive spectrometers were used for the measurements. Thallium acid phthalate and pentaerythritol crystals were used to measure Zr and U, respectively. Each element was measured for 60 s using 15 kV 30 nAs in spot mode. The measurements were taken on the peak center and on the two backgrounds. A linear background subtraction was used to calculate the peak/background. A thin layer of graphitic carbon was evaporated onto the samples and standards for electrical conductivity.

The K-ratio for each element was determined and a PHI-X ZAF correction for the matrix was performed. The K-ratio is the counts per nAs measured at the peak center for the sample divided by the same measurement on the standard. The standard calibration is actually the average of 3-4 separate measurements. Each K-ratio is given a ZAF correction which is an attempt to model the effects of the matrix upon the measured X-ray signal. For similar measurement conditions, such as the thickness of carbon coating, degree of oxidation, and beam current, the sum of the corrected K-ratios should add up to 100%. This assumes that the ZAF correction that models the effects of the matrix is correct. Counting statistics determine the precision of the technique, but the accuracy is primarily a function of standards and ZAF corrections. For these types of measurements a 1% accuracy can be expected.

## **4.0 RESULTS AND DISCUSSION**

### **4.1 Flatness and Microstructure**

The foils were reduced to a final thickness of 0.38 mm (0.015 in) by hot and cold rolling. Final foil lengths were typically ~686 mm (27 in.). Figure 3 displays the thickness at each pass, for the set of foils that were annealed at 650°C. Thickness at each pass plots for the other annealing temperatures can be found in Appendix A. The jumps in thickness after passes 10-20 indicate the transition from hot to cold rolling. As mentioned in Section 3.1, the actual foil thickness could not be determined during hot rolling due to the presence of the can. Therefore the foil thickness was calculated from the measured overall can thickness, assuming that foil and can deformation were proportional. The actual foil thickness after hot rolling was measured after the foil was removed from the can. Actual strain was also calculated after the foil was removed from the can.

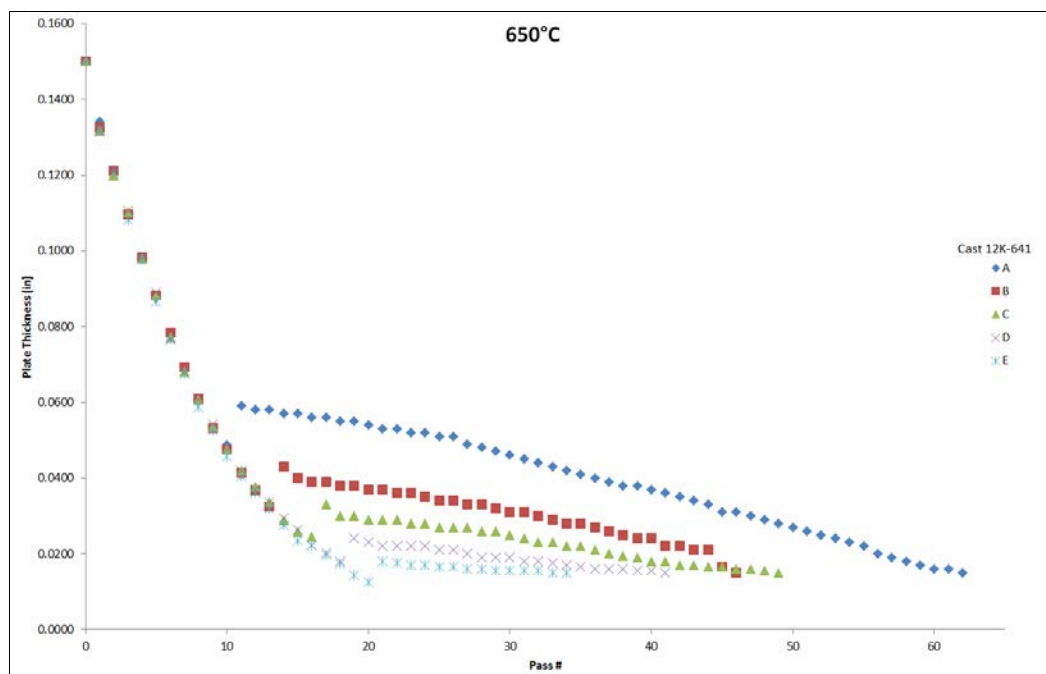


Figure 3: Thickness at each pass during hot and cold rolling for foils annealed at 650°C. Jumps in the thickness at 10-20 passes indicate the transition from hot to cold rolling.

Table 2 gives the foil IDs for each combination of hot rolling, cold rolling, and annealing temperature. Some extremes in hot and cold rolling were not performed, once initial results showed that these processing parameters resulted in unsatisfactory foils. A total of 22 processing parameters were performed.

			Annealing Temperatures (°C)				
Nominal Processing Parameters	%HR	%CR	550	600	650	700	750
	91	5	Not Processed	652-E	641-E	644-E	Not Processed
	88	29	643-F	652-D	641-D	644-D	643-C
	82	50	643-E	652-C	641-C	644-C	643-B
	75	65	643-D	652-A	641-B	644-B	643-A
	65	75	644-F	652-B	641-A	644-A	Not Processed

Table 2: Foil IDs for all rolling and annealing combinations.



Figure 4 displays a typical set of foils that underwent different levels of hot and cold rolling based on the calculations shown in Table 1. Images of all the hot and cold rolled foils can be found in Appendix A. Surface roughness after hot rolling was mirrored on the inner surface of the cans they were hot rolled in. The surface roughness actually improved with increased hot rolling. It was determined that the lowest level of hot rolling (~65% reduction of thickness) failed to properly bond the Zr layers to the DU-10Mo, which resulted in blisters and other surface defects as shown in Figure 5. A minimum amount of 75% reduction of thickness by hot working is required to successfully bond the Zr to the DU-10Mo.

Cold rolling 25-75% significantly improved the smoothness and flatness of the foils. Cold rolling 5% was not sufficient to remove the surface roughness or greatly improve the flatness. It was determined that 75% hot rolling is needed to avoid blisters and a minimum amount of 50% cold working is required to improve the surface conditions of the foils.

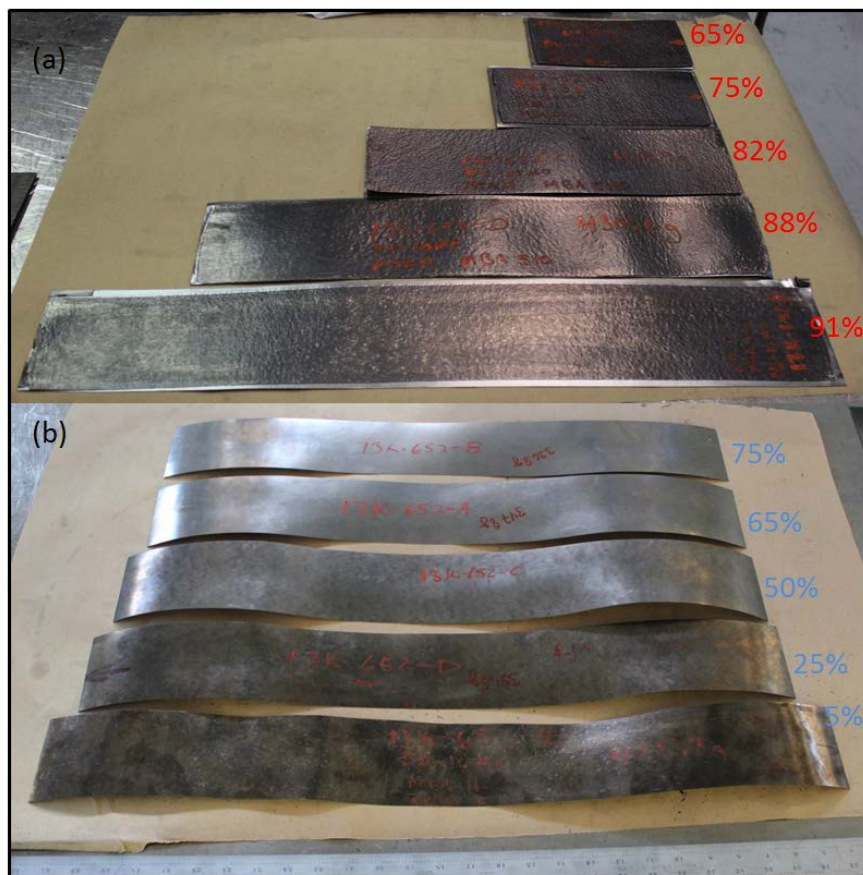


Figure 4: Foils 13K-652 A-E. (a) Foils after hot rolling. Surface roughness improves with increased hot reduction. (b) Foils after cold rolling. Surface smoothness improves with increased cold rolling.

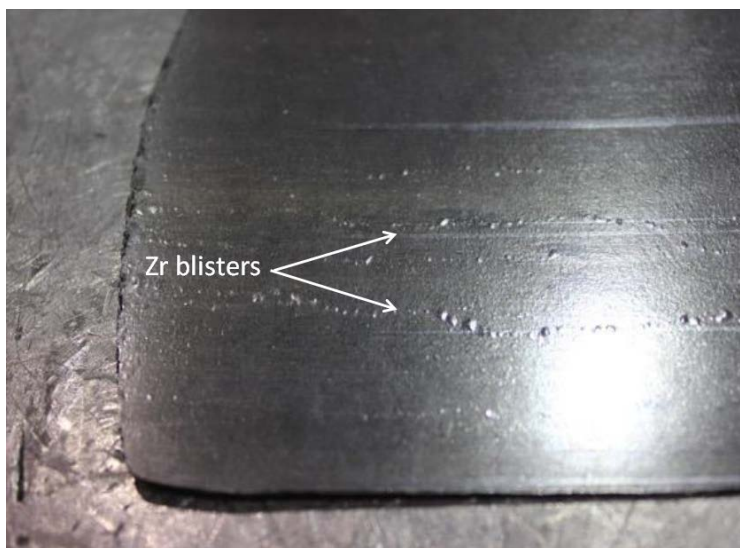


Figure 5: Surface blisters and defects due to inadequate bonding between the Zr and U-10Mo during hot rolling. The minimum hot reduction of 65% is not acceptable for this application.

For the annealing procedure, the foils were sandwiched between two copper plates. An additional mass was placed on top of the upper copper plate, for a total mass of ~40 kg. Figure 6 displays a typical example of the pre-annealed foils, the weighted plates, and the post-annealed foils. Using the weighted vacuum annealing process was successful at removing most or all of the bows and ripples from the foils. The Cu plates were slightly distorted by the annealing process, but overall the DU-10Mo foils were much flatter than before annealing. In general, annealing at temperatures of 650°C or higher dramatically improved the flatness of the foils.

Oil quenching was immediately performed after vacuum annealing to prevent any possible phase transformations from occurring. This is necessary because DU-10Mo has a metastable microstructure and can decompose if held at higher temperatures. Quenching preserves the gamma phase and prevents the DU-10Mo from decomposing.

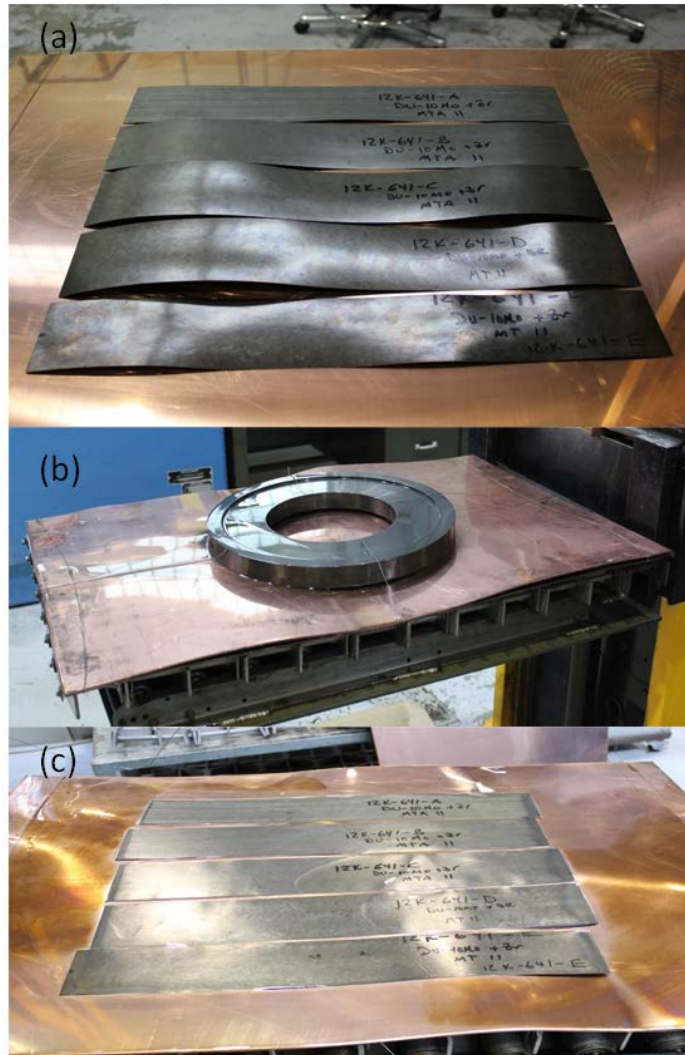


Figure 6: Vacuum annealing at 650°C. Annealing improves flatness and uniformity. (a) As-cold-rolled foils, (b) Foil sheets sandwiched between the Cu plates and weighted, and (c) Foils after annealing show overall improved flatness. Some distortion of the Cu plates occurred.

Metallographic examination investigated the effects of annealing treatments on the microstructure and on the interface between the Zr and the DU-10Mo. Figure 7 shows examples of sections of foils that underwent annealing at 600-750°C. The micrographs revealed that Zr, U, and Mo interact during the rolling process and annealing treatments to form reaction layers that contain diffusion gradients, numerous reaction products, and Mo-enriched and Mo-depleted regions. These reaction layers were complex, irregular, and varied greatly in thickness locally. Figure 8 displays a better view of the irregularity and varied thickness of the reaction layer for a foil annealed at 600°C. Example views of the interaction zones from foils at all annealing temperatures can be found in Appendix B.

Micrographs also showed that recrystallization occurred in the DU-10Mo material, for some of the rolling and annealing conditions. Recrystallization of the DU-10Mo was also confirmed by EBSD (discussed below).



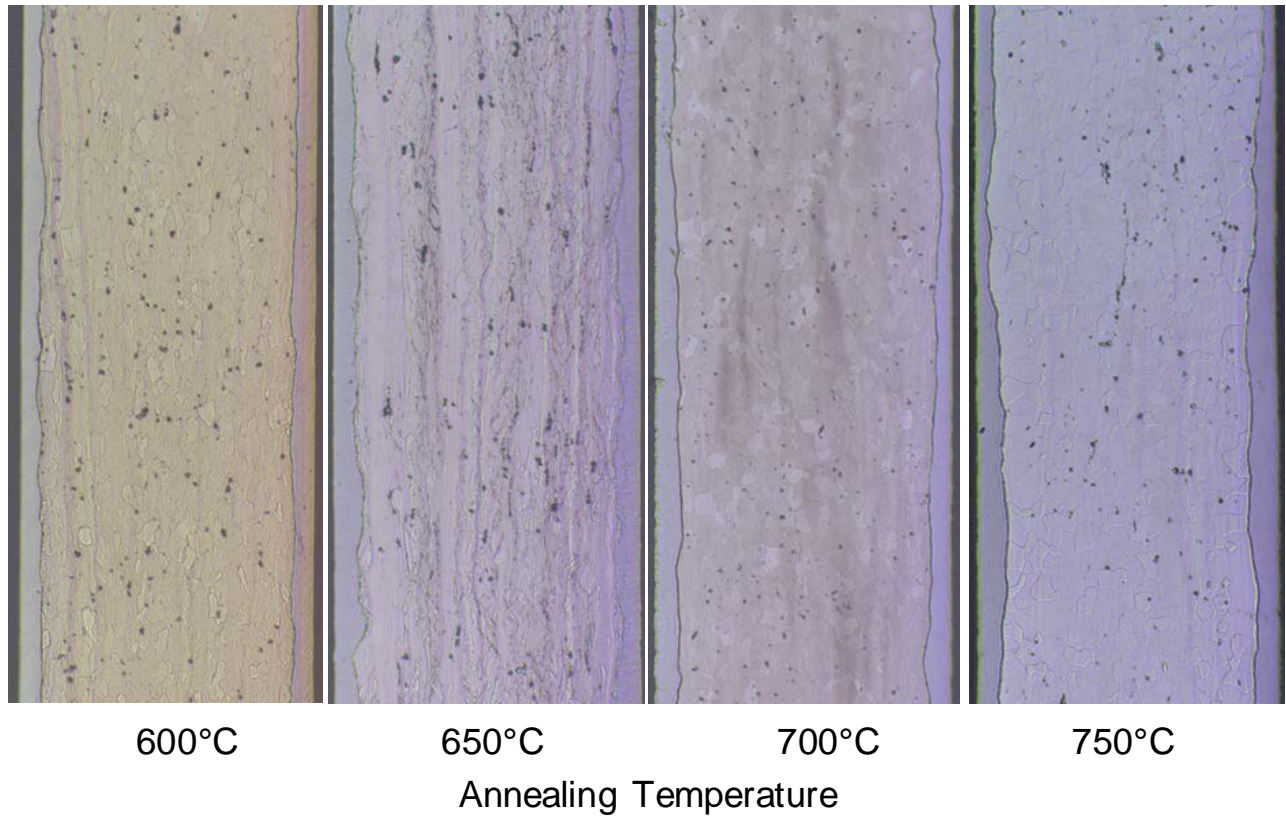


Figure 7: Light optical microscopy taken at 100X magnification. Microstructures of sections through annealed foils. Note the variable thickness of the Zr layer on the edges of the foils.

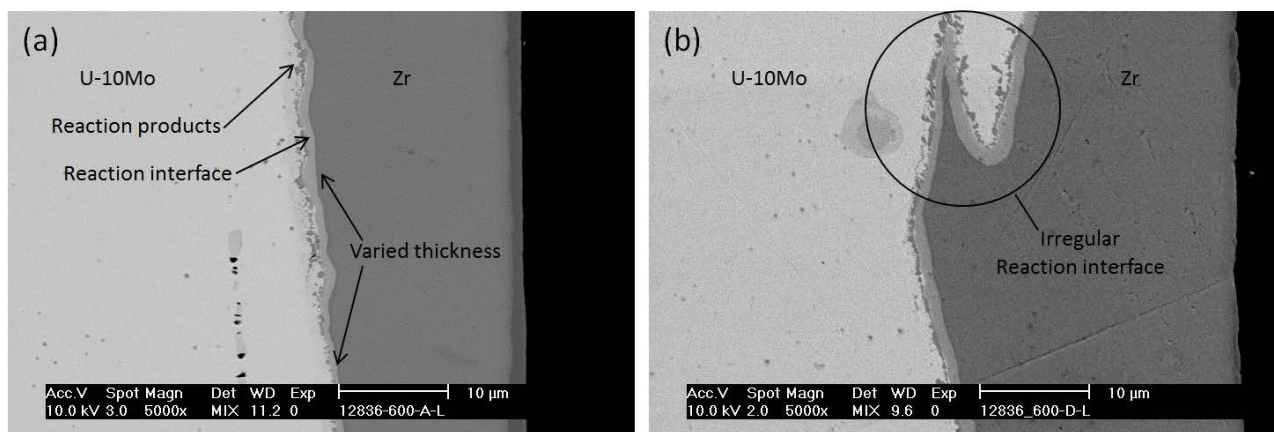


Figure 8: SEM images showing interaction zones for foils annealed at 600°C. (a) Foil 652-A, 65% CR, and (b) Foil 652-D, 29% CR. The Zr appears dark, and the (DU-10Mo) is light.

LOM showed the pancake grain structures of the foils caused by cold rolling. The pancake grain structures were prominent for foils that underwent annealing at 550°C and 75-65% cold rolling. The grain orientation indicated the direction of rolling of the foils. Very little recrystallization occurred for annealing at 550°C. LOM also showed that the grain structures of several foils annealed at higher temperatures underwent recrystallization. When annealing at 700°C, the grain structures became more refined as cold rolling increased. This was not the general trend when annealing at 750°C. The average grains sizes could only be derived for 700-750°C annealing temperatures, where full recrystallization occurred. Lower annealing temperatures produced microstructures with a significant fraction of un-recrystallized grains. These grains were very long in the rolling direction. The average grain sizes, for the foils annealed at 700 or 750°C, as reported by the EBSD software (diameter of circular grains of equivalent area) are shown in Figure 9.

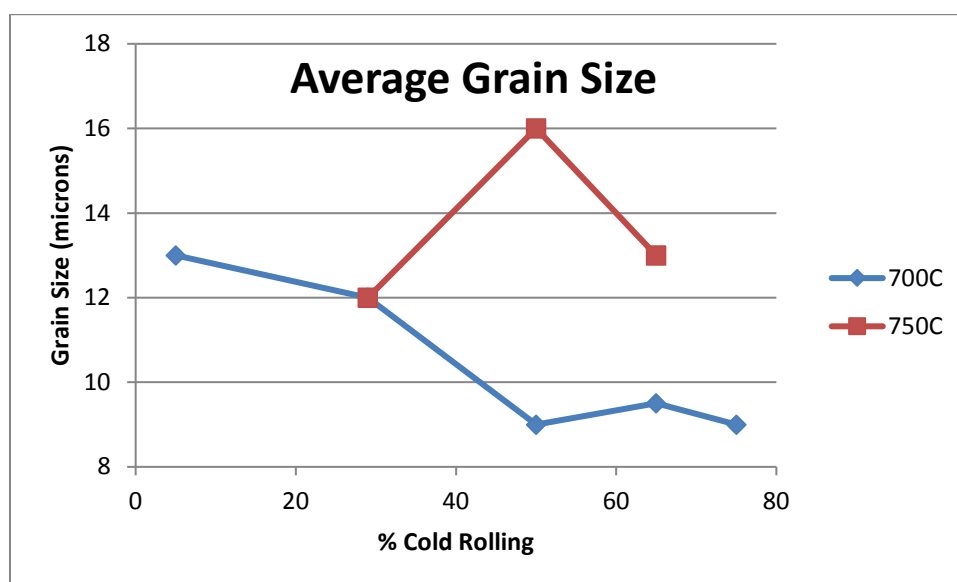


Figure 9: Grain sizes for annealing temperatures of 700 and 750°C.

EBSD confirmed that annealing at higher temperatures resulted in more recrystallization. Figure 10 shows the EBSD results for foils annealed at 700°C. The complete set of the available EBSD data can be found in Appendix C. The EBSD results are presented in 3 forms. The top layer shows texture intensity pole figures, with a color scale in number of times random intensity. The middle row of images shows the inverse pole figure (IPF) map, in the transverse direction (TD), with the orientations shown by the orientation triangle. The rolling direction (RD) and through-thickness (TT) orientations are shown. The lower row of images are the grain orientation spread (GOS) results, with the color scale shown in degrees.

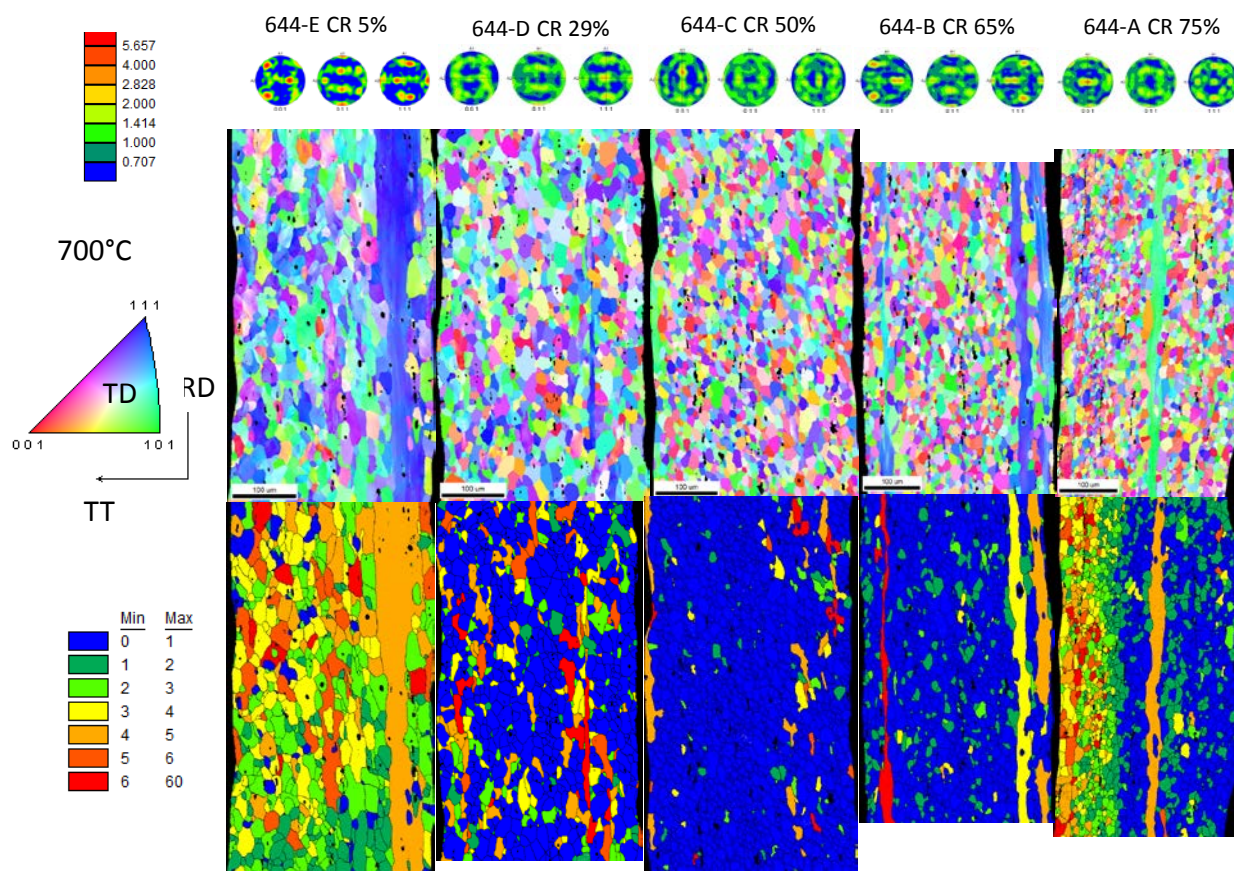


Figure 10: EBSD results of foils annealed at 700°C. Top row: texture intensity pole figures. Middle row: inverse pole figure maps. Bottom row: Grain Orientation Spread maps.

Annealing at 550°C (Figure C1) for 1 hour resulted in very little recrystallization. The texture is very similar to rolling textures of other body center cubic (BCC) metals. For 600°C (Figure C2), there is no or very little recrystallization for the lower levels of cold rolling (5 or 29%), while there is only partial recrystallization for higher levels of cold rolling. More recrystallization is evident for annealing at 650°C (Figure C3), although the results are inconsistent, and this set of data is therefore regarded as suspect, particularly for the higher rolling levels.

Recrystallization is very evident for annealing at 700°C (Figure C4), for cold rolling at 29% or more. Similarly, full recrystallization occurs with annealing at 750°C (Figure C5). As noted previously, the grain sizes obtained with annealing at 750°C are slightly greater than those obtained for similar rolling conditions, but annealed at 700°C. Cold rolling to only 5% is usually not enough strain to prompt recrystallization, at least up to 700°C. No foil was processed with only 5% cold rolling for annealing at 750°C, so it is not known if recrystallization would occur for this strain-temperature combination.



## 4.2 U, Zr and Mo Profiles

EDS was used to measure the elemental weight percent of Zr, U, and Mo, across the (DU-10Mo)-Zr interface. Zr is present at 100% in the Zr layer, while the U and Mo weight percentages rise to and plateau at 90 and 10%, respectively, in the DU-10Mo material; there are gradients in these elements across the interface region. Figure 11 displays a typical set of elemental weight percent versus distance plots across the (DU-10Mo)-Zr interface region for a sample annealed at 550°C. Examples from all annealing temperatures can be found in Appendix D. At least two line scans per sample were obtained.

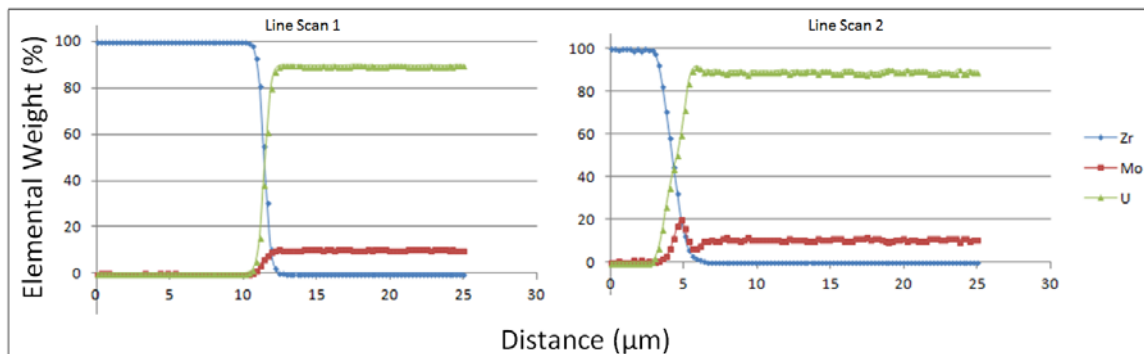


Figure 11: EDS line scans for foils annealed at 550°C.

## 4.3 Microhardness

Vickers microhardness measurements showed that the hardness of the foils generally decreased with increasing annealing temperature. Figures 13 and 14 display the Vickers microhardness trends that were obtained in the longitudinal and transverse orientations, respectively. Foils that were 50-65% cold rolled exhibited the greatest hardness at 550°C. In the longitudinal orientation, the trend plateaus off to ~284 at 700-750°C. There was no distinct or plateauing trend in the transverse orientation.

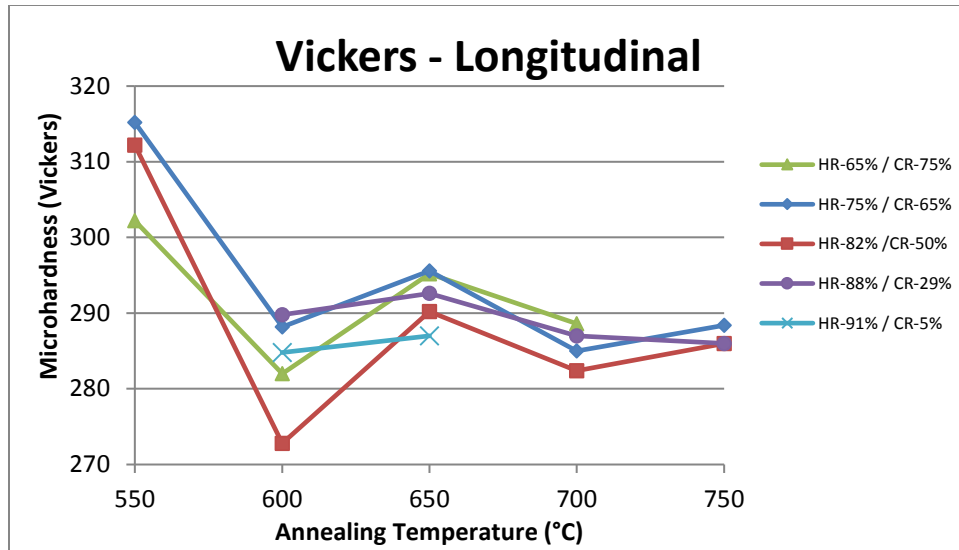


Figure 13: Vickers Microhardness as a function of annealing temperature, for samples taken in the longitudinal orientation.

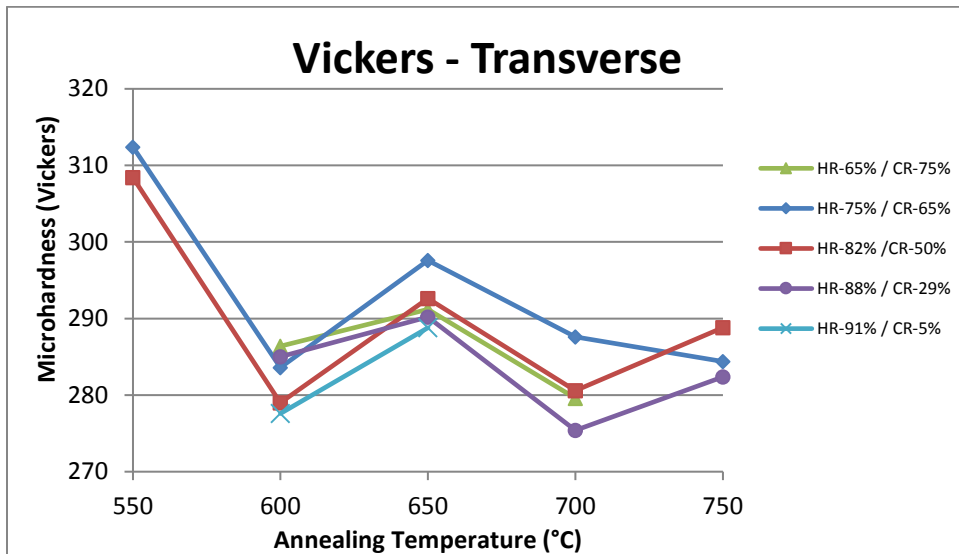


Figure 14: Vickers Microhardness as a function of annealing temperature, for samples taken in the transverse orientation.

## 5.0 CONCLUSION

This work has demonstrated that the vacuum annealing process can greatly improve flatness and reduce waviness in the (DU-10Mo)-Zr foils. HIPing the (DU-10Mo)-Zr foils to the Al cladding can be performed at a higher level of confidence knowing that the final alignment will not be

affected due to waviness, and the proper thickness and flatness should be consistently achievable. Conclusions are as follows:

1. A minimum of 75% reduction in thickness, by hot rolling, is required to successfully bond the Zr to the DU-10Mo fuel.
2. A minimum of 25% (preferably 50%) reduction in thickness, by cold rolling, is needed to smooth out the rough, irregular surface resulting from hot rolling.
3. A simple vacuum annealing process, with the foils constrained between weighed Cu sheets, can help to significantly improve the flatness of cold-rolled foils.
4. All annealing temperatures (550-750°C) were able to reduce the waviness of cold-rolled foils. Foils are not completely flat.
5. Recrystallization occurs at 700°C and above. Annealing at 700°C or higher is recommended if full recrystallization is desired.
6. An interaction layer develops at the (DU-10Mo)-Zr interface. This layer is complex and variable, but generally increases in width as the annealing temperature increases. Mo-enriched and Mo-depleted regions generally develop in the interaction zone.

## ACKNOWLEDGEMENTS

The authors would like to acknowledge the financial support of the U.S. Department of Energy (DOE) National Nuclear Security Administration (NNSA) Office of Materials Management and Minimization (M3) Reactor Conversion Program. Los Alamos National Laboratory, an affirmative action equal opportunity employer, is operated by Los Alamos National Security, LLC, for the NNSA of the U.S. DOE under contract DE-AC52-06NA25396.

## REFERENCES

- [1] D. J. Alexander, K. D. Clarke, J. E. Scott, J. D. Montalvo, and D. E. Dombrowski, Effect of Cold Deformation and Annealing Temperature on U-10Mo Fuel Foil Geometry, LA-UR-14-21384, RRFM 2014 European Research Reactor Conference, Ljubljana, Slovenia, March 30 – April 3, 2014
- [2] D. E. Dombrowski, R.M. Aikin, K.D. Clarke, T. Lienert, P.O. Dickerson, L.A. Tucker, D. A. Summa, D. J. Alexander, M. Hill, LANL Progress on U-Mo Fuel Fabrication Process Development, LA-UR-14-27697, RERTR 2014 — 35th INTERNATIONAL MEETING ON REDUCED ENRICHMENT FOR RESEARCH AND TEST REACTORS' OCTOBER 12-16, 2014, IAEA VIENNA INTERNATIONAL CENTER, VIENNA, AUSTRIA, page 8
- [3] R. E. Reed-Hill and R. Abbaschian. Physical Metallurgy Principles. 3<sup>rd</sup> Edition. 1992. PWS-Kent.
- [4] W. D. Callister, Jr. and D. G. Rethwisch. Materials Science and Engineering: An Introduction. 7<sup>th</sup> Edition. 2007. John Wiley & Sons, Inc.

[5] M. Krzyzanowski, J. H. Beynon, and D. C. J. Farrugia. Oxide Scale Behavior in High Temperature Metal Processing. 1<sup>st</sup> Edition. 2010. John Wiley & Sons, Inc.

[6] F. C. Campbell. Metals Fabrication: Understanding the Basics. 1<sup>st</sup> Edition. 2013. ASM International.

[7] R. M. Aikin, Jr., personal communication, LANL, 2013

## Appendix A

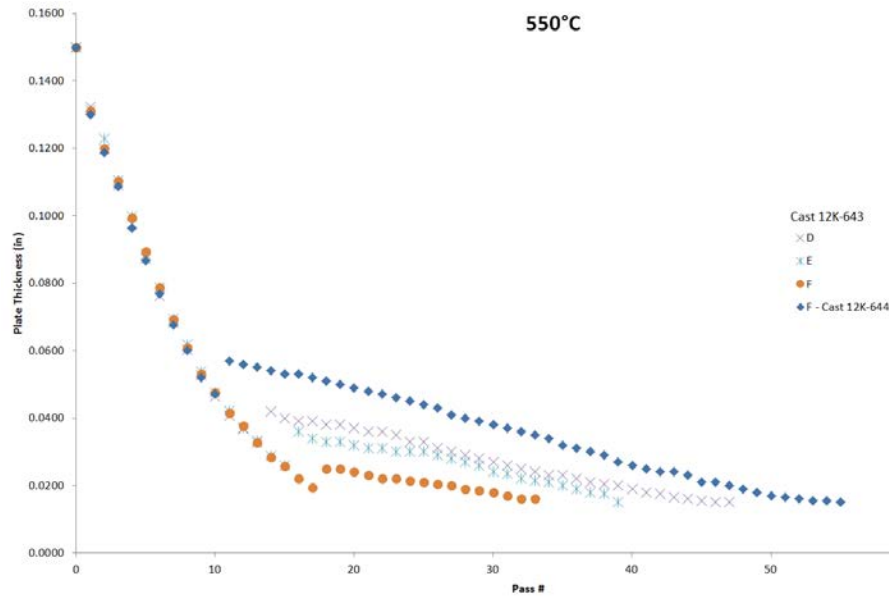


Figure A1: Thickness at each pass during hot and cold rolling for foils annealed at 550°C.

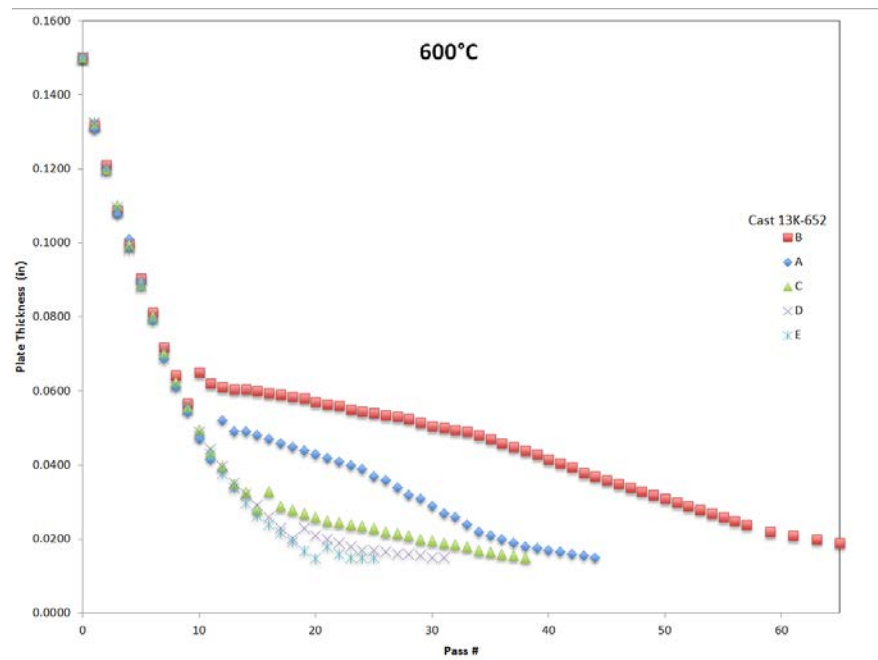


Figure A2: Thickness at each pass during hot and cold rolling for foils annealed at 600°C.



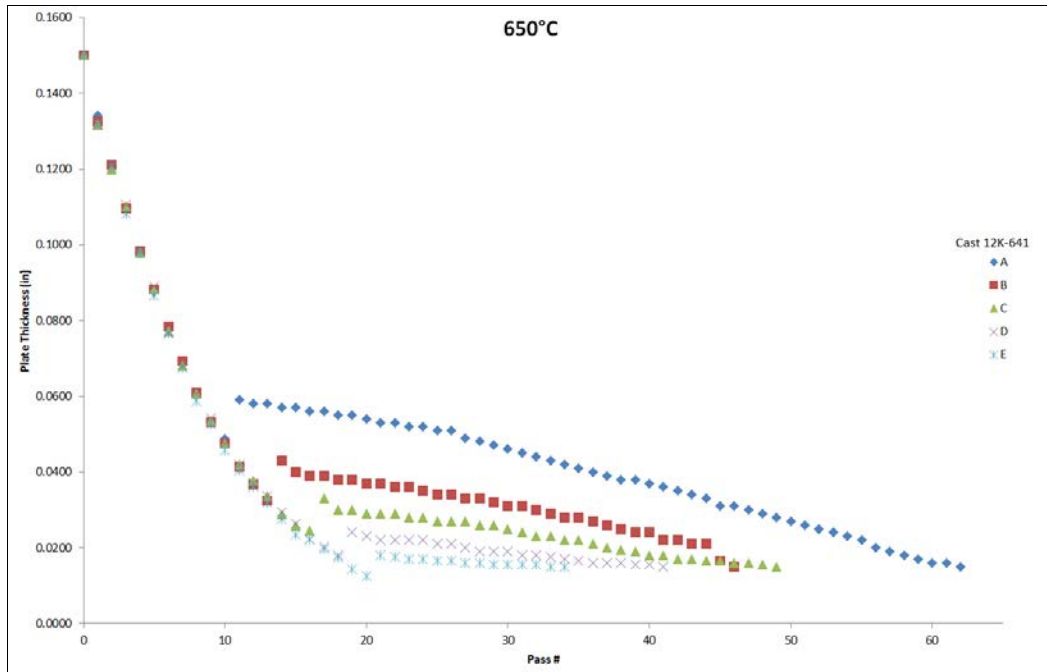


Figure A3: Thickness at each pass during hot and cold rolling for foils annealed at 650°C.

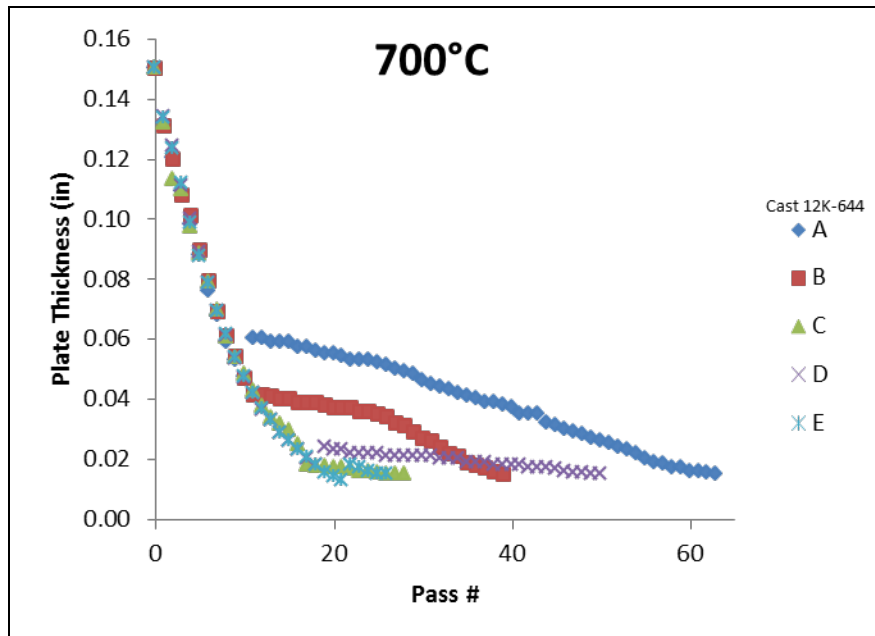


Figure A4: Thickness at each pass during hot and cold rolling for foils annealed at 700°C.

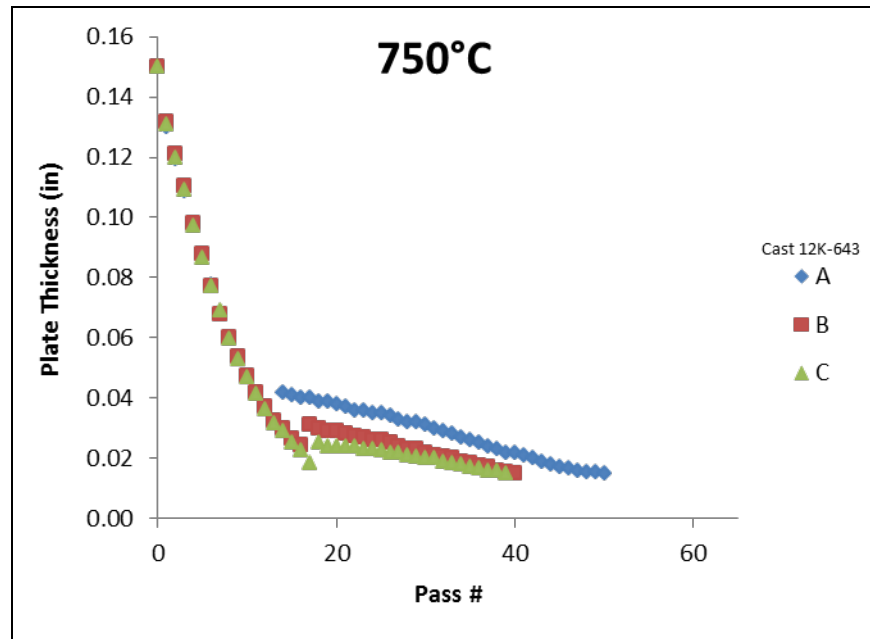


Figure A5: Thickness at each pass during hot and cold rolling for foils annealed at 750°C.

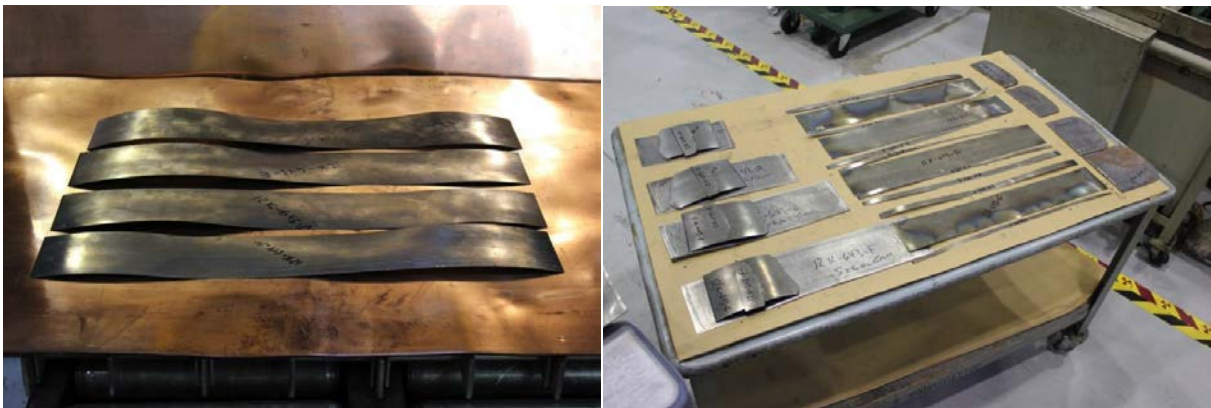


Figure A6: Foils before and after vacuum annealing at 550°C.

UNCLASSIFIED

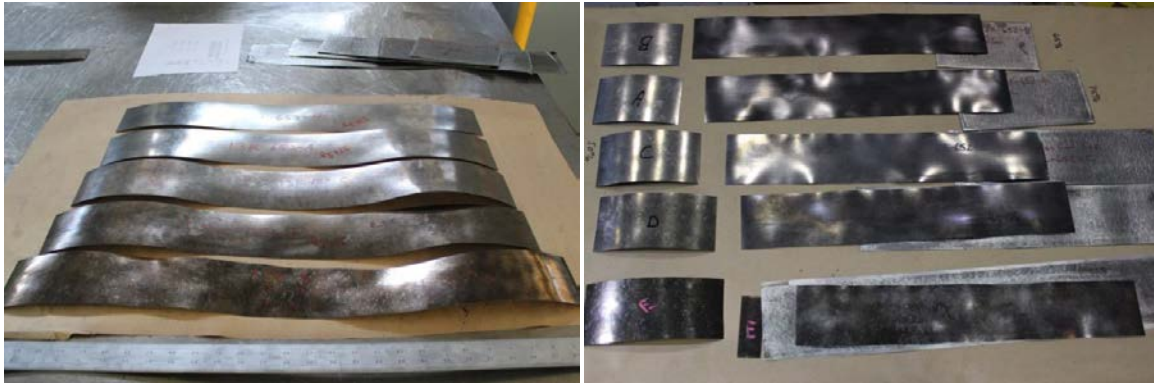


Figure A7: Foils before and after vacuum annealing at 600°C.

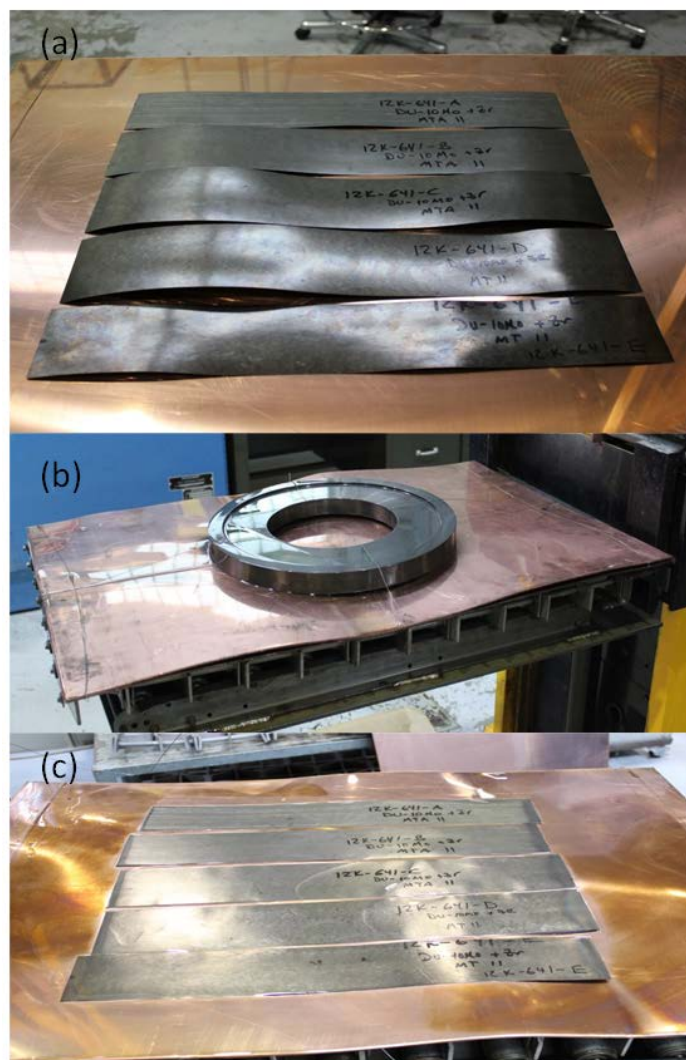


Figure A8: Foils before and after vacuum annealing at 650°C.

UNCLASSIFIED



Figure A9: Foils before and after vacuum annealing at 700°C.



Figure A10: Foils before and after vacuum annealing at 750°C.



## Appendix B

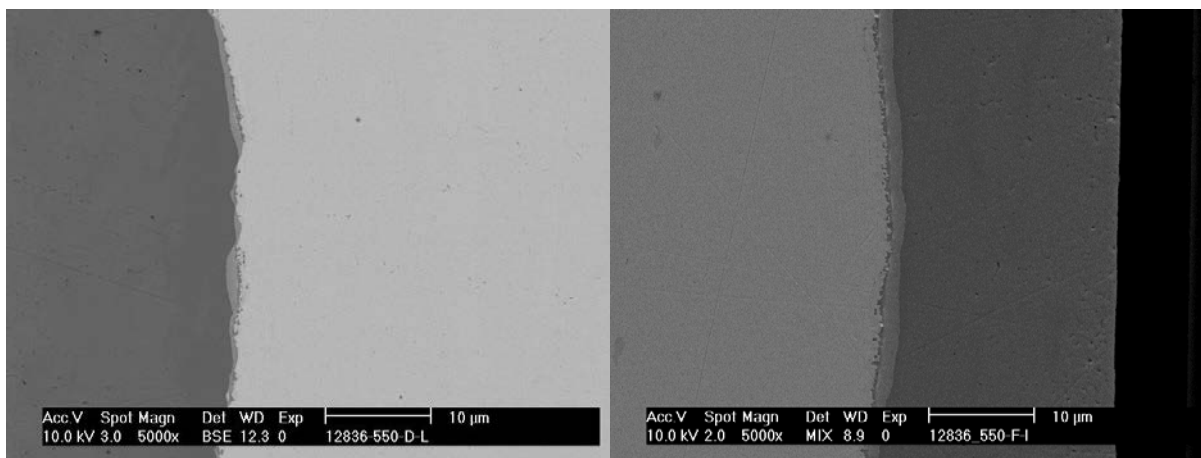


Figure B1: Interaction zones of foils 643-D (left) and 644-F (right) annealed at 550°C. Zr appears dark, (DU-10Mo) is light.

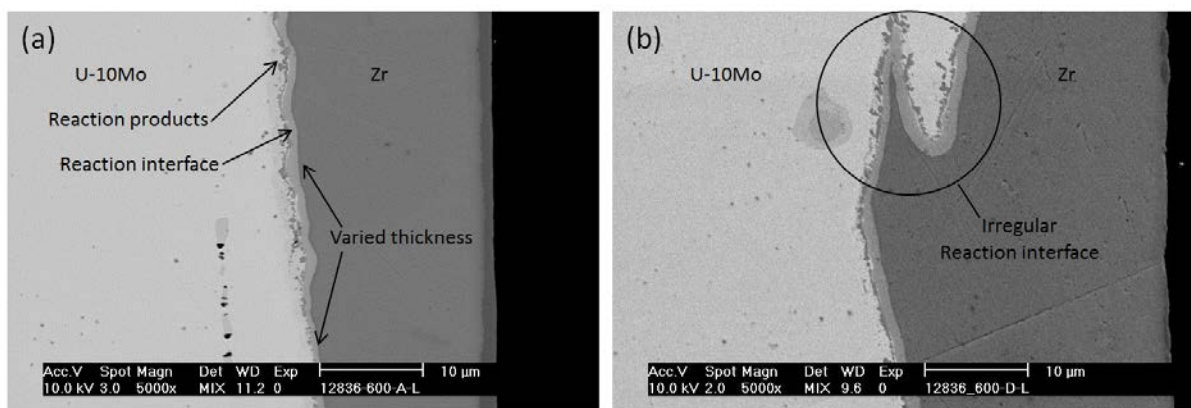


Figure B2: Interaction zones for foils annealed at 600°C. (a) Foil 652-A with 65% CR, and (b) Foil 652-D with 29% CR. Zr appears dark, (DU-10Mo) is light.

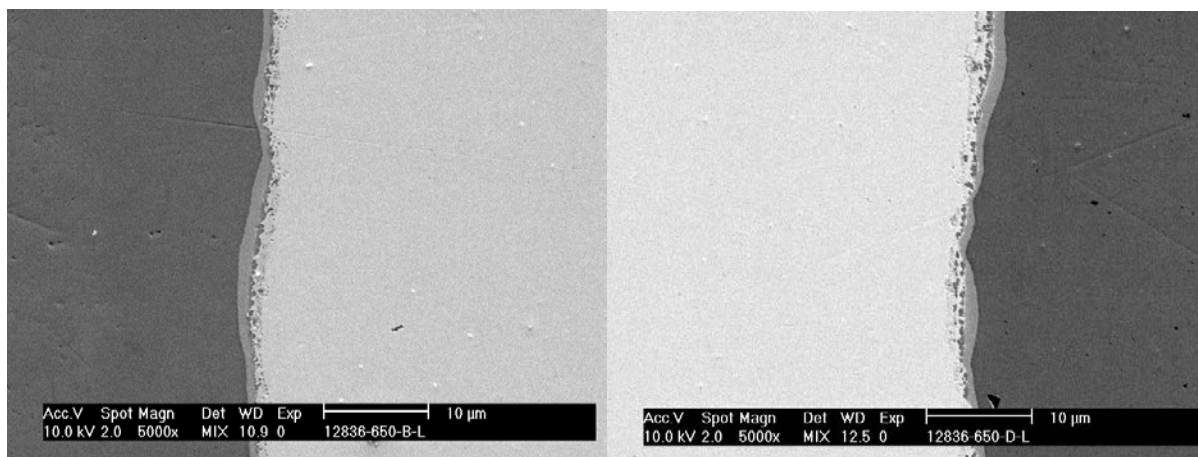


Figure B3: Interaction zones for foils 652-B (left) and 652-D (right) annealed at 650°C.  
Zr appears dark, (DU-10Mo) is light.

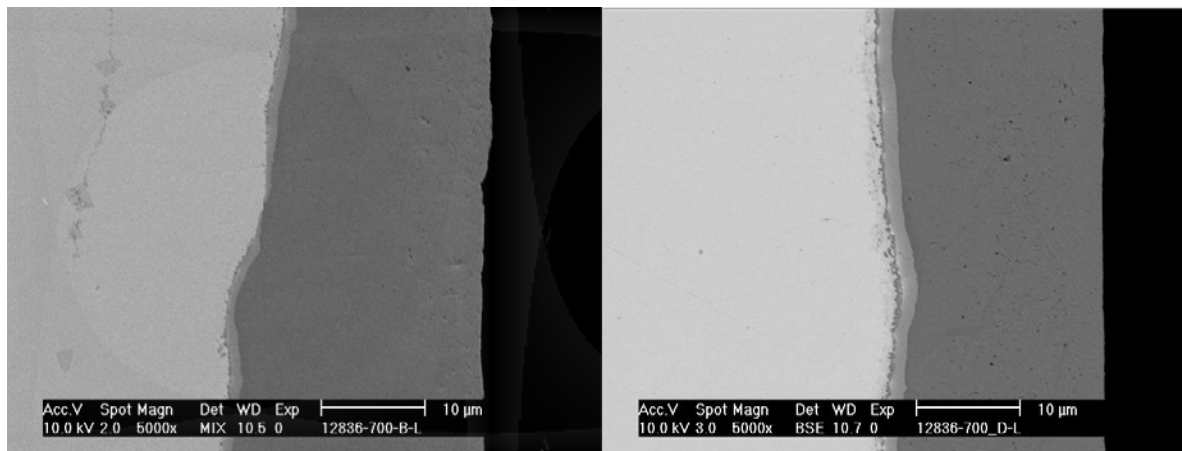


Figure B4: Interaction zones of foils 644-B (left) and 644-D (right) annealed at 700°C.  
Zr appears dark, (DU-10Mo) is light.

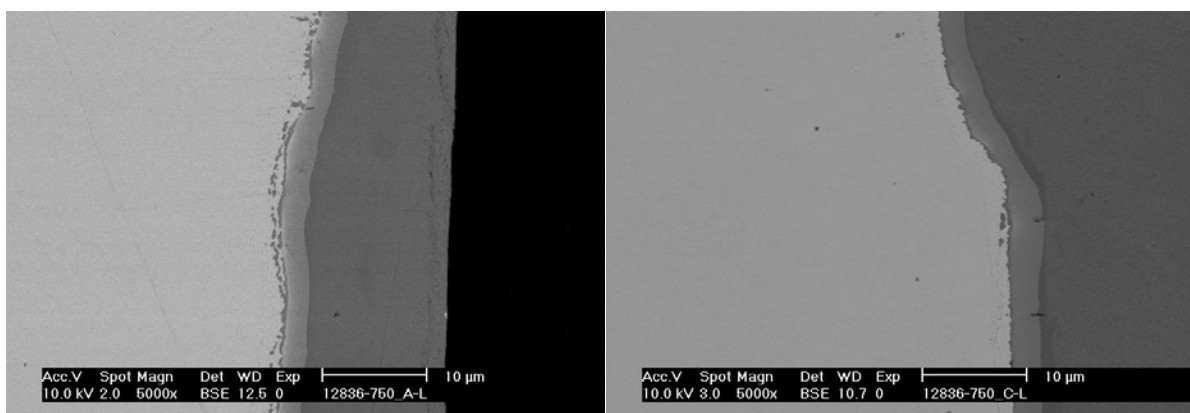


Figure B5: Interaction zones of foils 643-A (left) and 643-C (right) annealed at 750°C.  
Zr appears dark, (DU-10Mo) is light.

## Appendix C

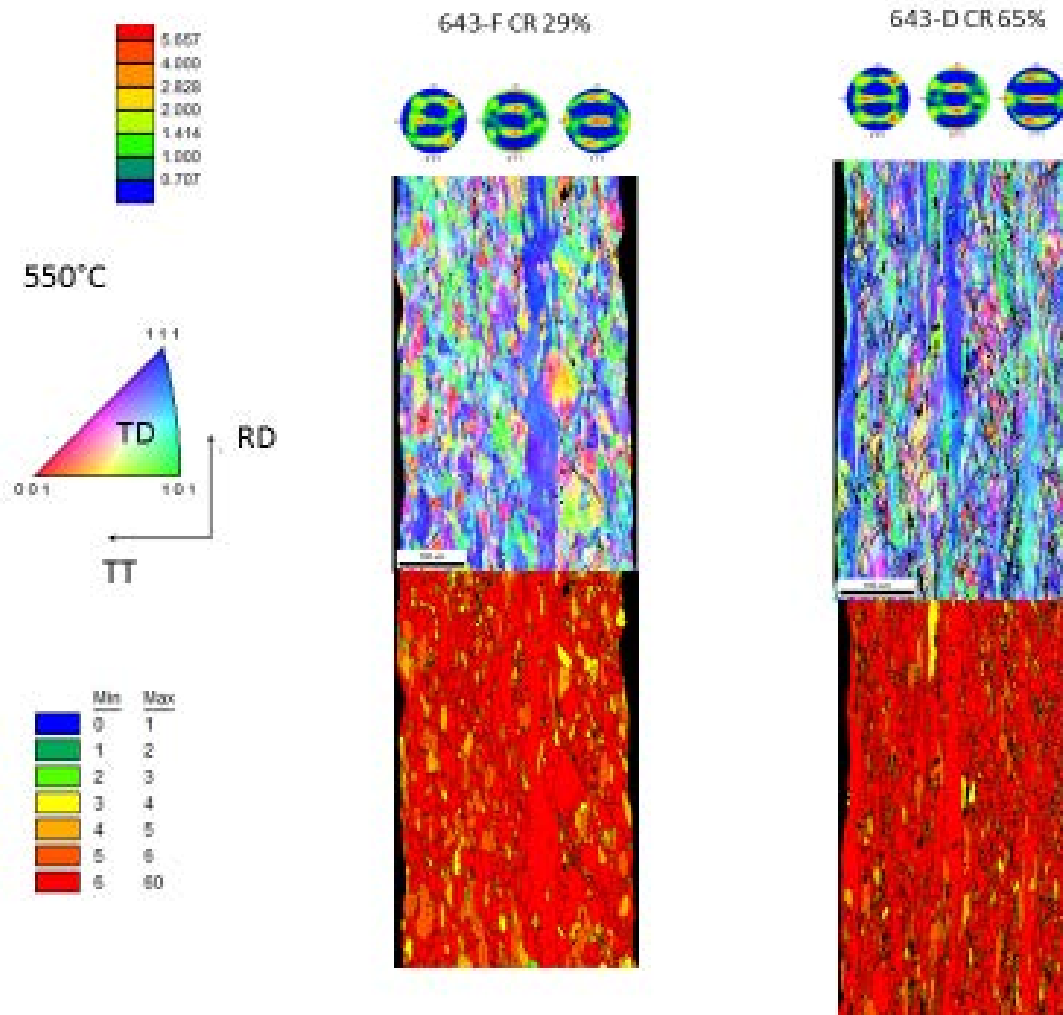


Figure C1: EBSD results for foils annealed at 550°C. Top row: texture intensity pole figures. Middle row: inverse pole figure maps. Bottom row: Grain Orientation Spread maps.



UNCLASSIFIED

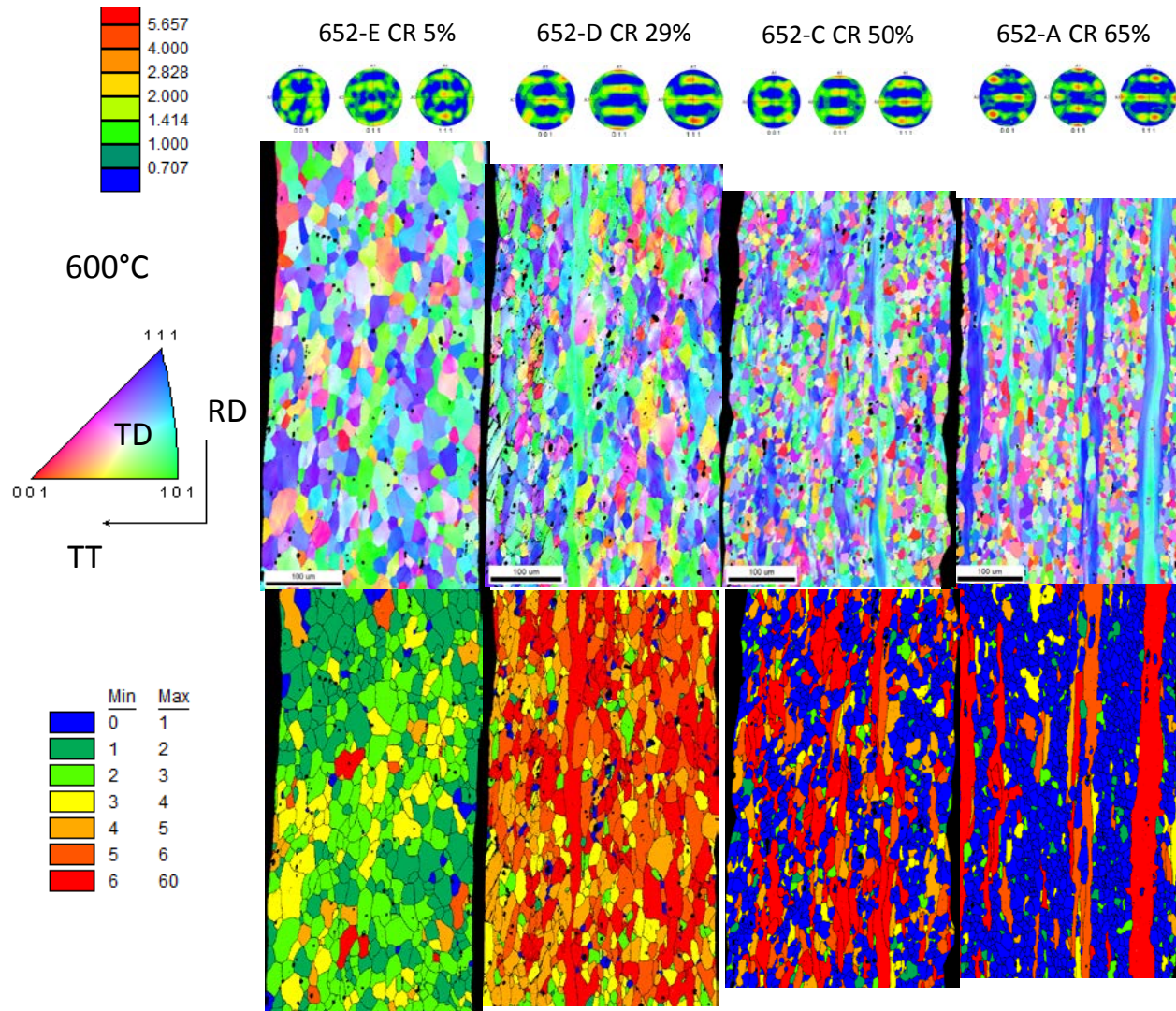


Figure C2: EBSD results of foils annealed at 600°C. Top row: texture intensity pole figures. Middle row: inverse pole figure maps. Bottom row: Grain Orientation Spread maps.

UNCLASSIFIED



UNCLASSIFIED

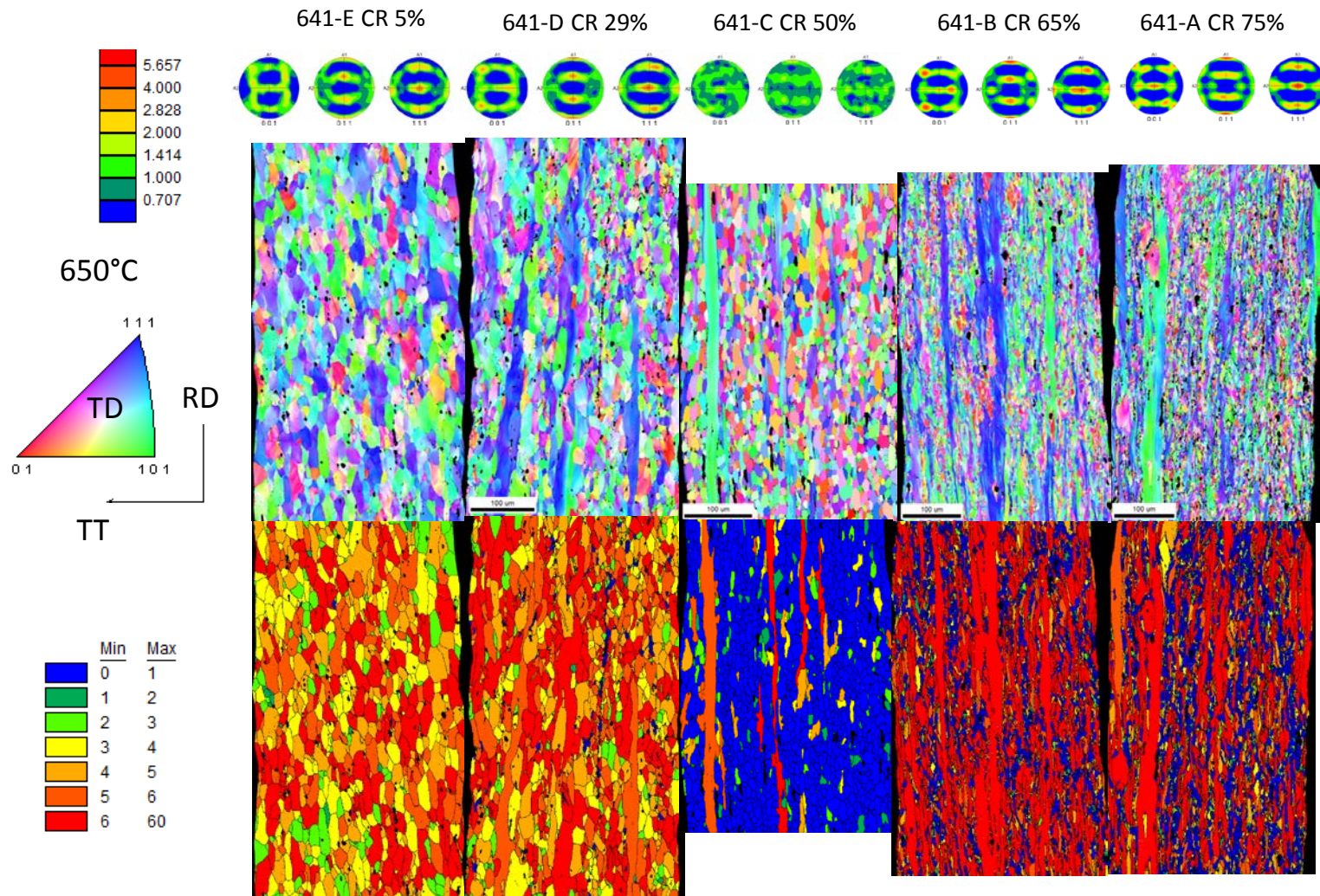


Figure C3: EBSD results of foils annealed at 650°C. Top row: texture intensity pole figures. Middle row: inverse pole figure maps. Bottom row: Grain Orientation Spread maps.

UNCLASSIFIED



UNCLASSIFIED

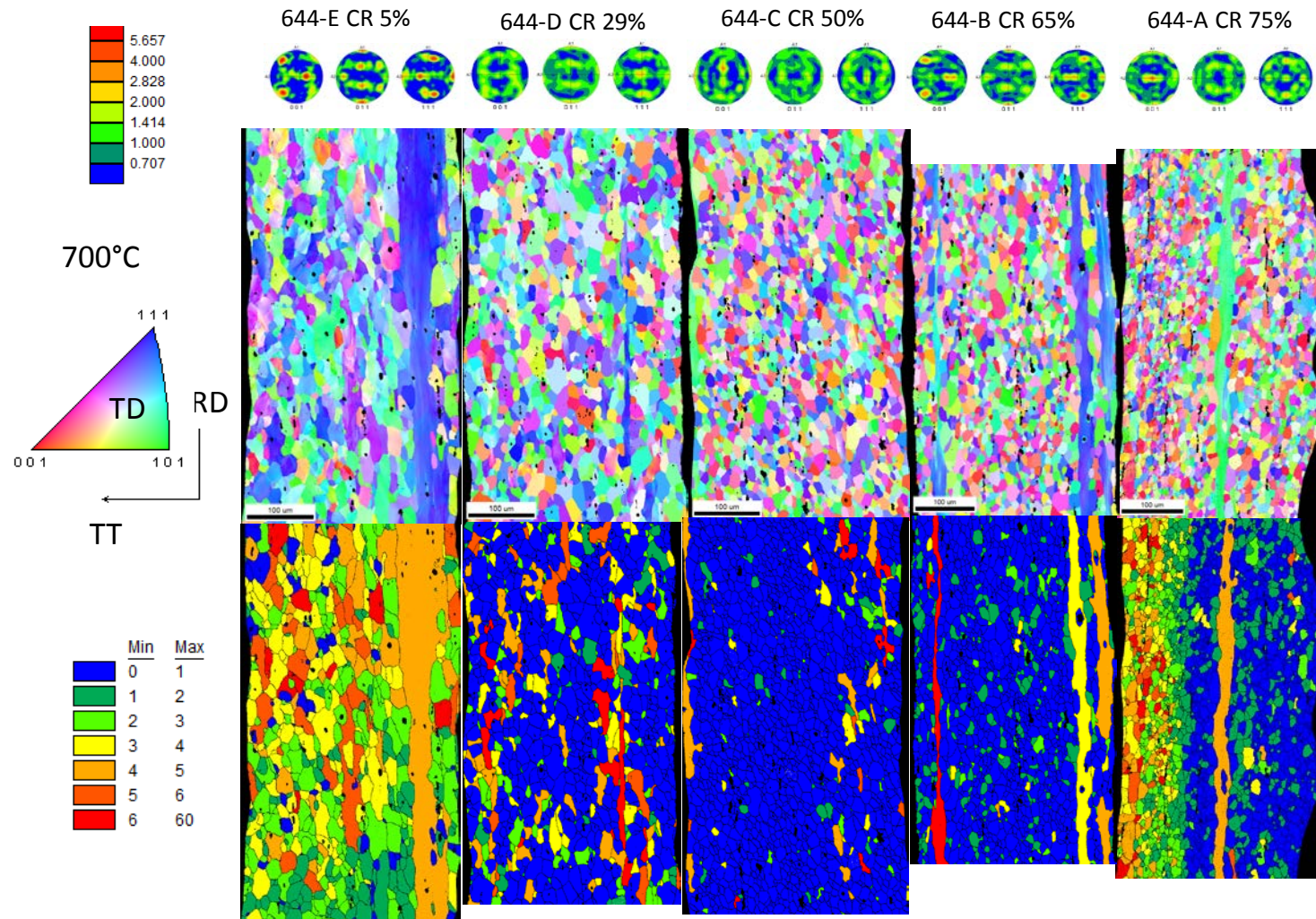


Figure C4: EBSD results of foils annealed at 700°C. Top row: texture intensity pole figures. Middle row: inverse pole figure maps. Bottom row: Grain Orientation Spread maps.

UNCLASSIFIED

UNCLASSIFIED

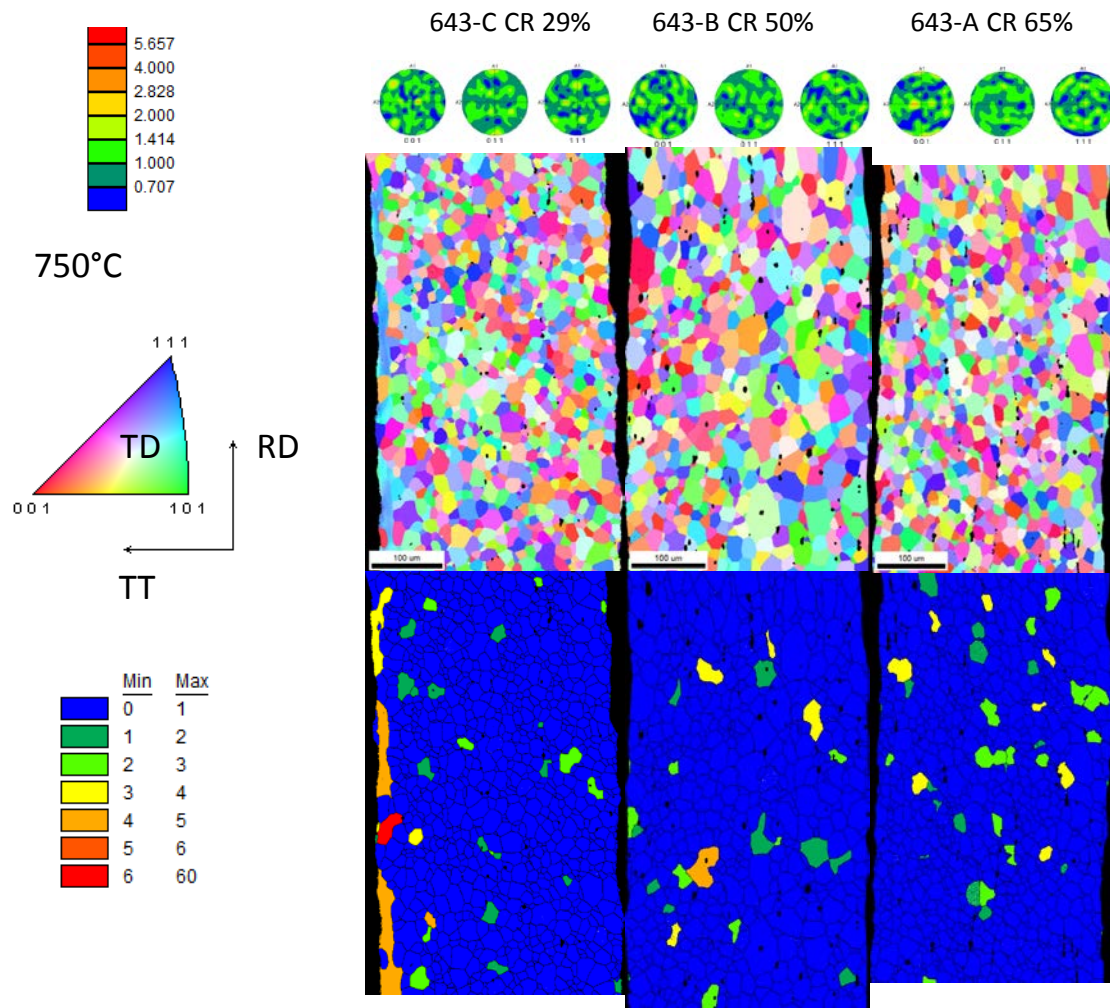


Figure C5: EBSD results of foils annealed at 750°C. Top row: texture intensity pole figures. Middle row: inverse pole figure maps. Bottom row: Grain Orientation Spread maps.

UNCLASSIFIED

## Appendix D

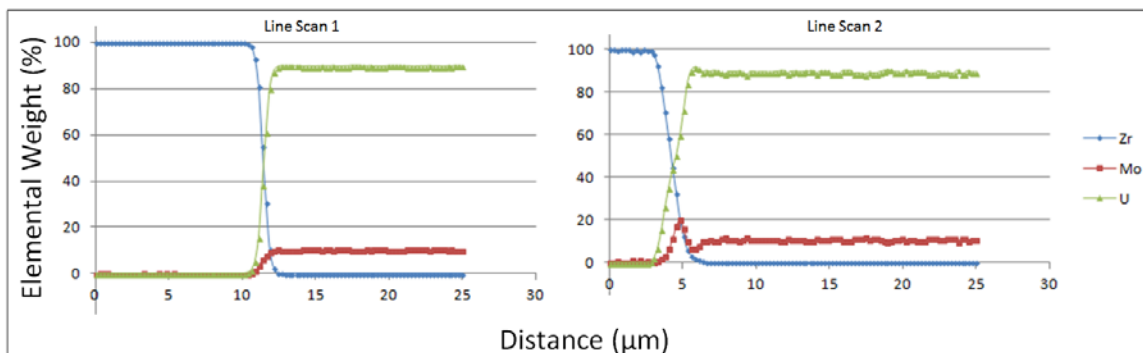


Figure D1: EDS line scans for foil annealed at 550°C.

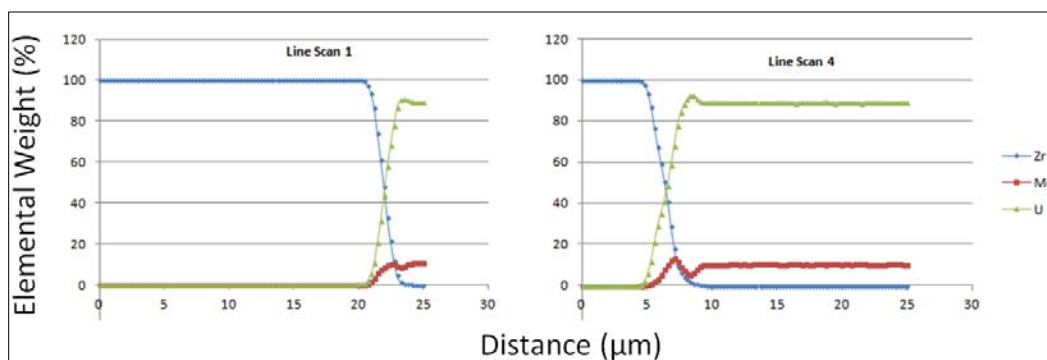


Figure D2: EDS line scans for foil annealed at 600°C.

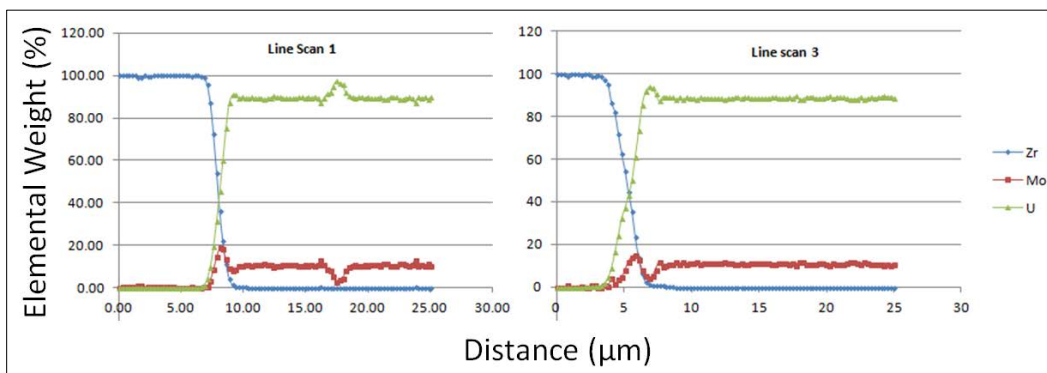


Figure D3: EDS line scans for foil annealed at 650°C.

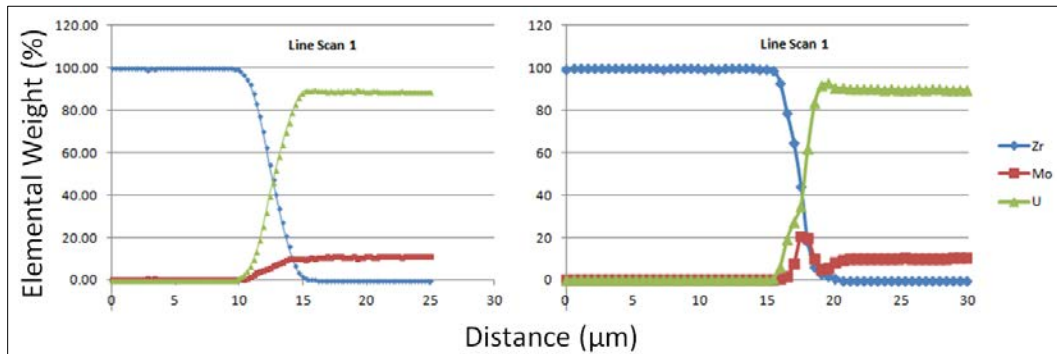


Figure D4: EDS line scans for foil annealed at 700°C.

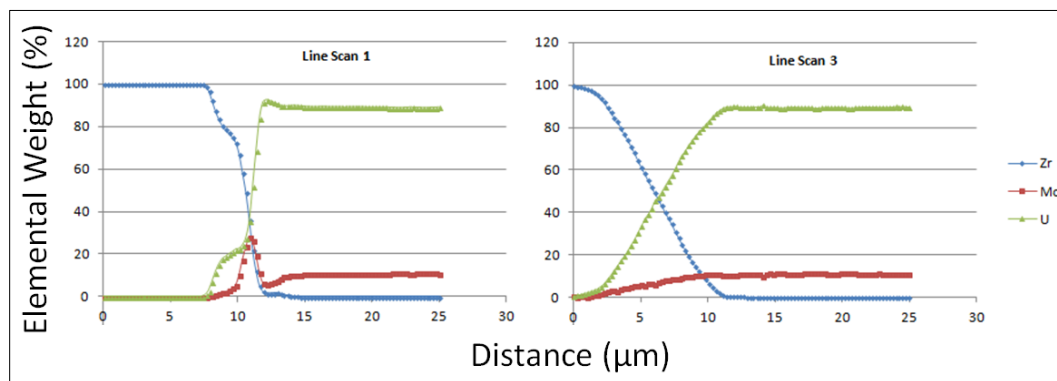


Figure D5: EDS line scans for foil annealed at 750°C.